PAPER

Check for updates

Protection of nickel by self-assembled monolayers prepared in an aqueous self-emulsifying solution of a novel amphipathic organothiol

Tao Yeyin, Li Xiaoya, Hou Peiming, Peng Shusen [ID] * and Ma Yongcun

This report explored a novel amphiphilic organothiol and prepared self-assembled monolayers (SAMs) on Ni substance in the aqueous micellar solution of this amphiphilic organothiol. The as-prepared amphiphilic organothiol can self-emulsify and disperse in an aqueous solution to form a stable emulsion without any additional emulsifier. The experiment shows that the self-emulsifying solution remains stable after six months at room temperature. The resulting SAMs are characterized by electrochemical measurements, XPS, porosity tests, and neutral salt spray experiments. XPS results show that the as-prepared self-emulsifying organothiol can bond to the Ni surface by forming strong thiolate Ni−S bonds. The electrochemical measurements show that the inhibition efficiency (η) and surface coverage (θ) increase with the immersion time in the aqueous micellar solution, reaching the maximum value of about 90 min. Experiments prove that AGE-CA SAMs provided better protection for Ni substances and electroplated Ni film than the OT SAMs from the ethanol solution.

1. Introduction

Self-assembled monolayers (SAMs) are organic ultrathin films that spontaneously form on metal surfaces and have the characteristics of a dense arrangement and stable structure.[1,2] Since Laibinis *et al.* demonstrated that organothiols can self-assemble on a Cu surface, protecting it from air oxidation;[3] SAM corrosion protection has attracted considerable attention as these do not affect the appearance and conductivity or thermal conductivity of the metal.[4,5] The commonly used organothiol is alkanethiol, structurally composed of a long *n*-alkane chain with a thiol group at one end. Upon adsorption, alkanethiols are reduced to alkanethiolates, and the alkane chain self-assembles into a more organized and insulating film, which provides a hydrophobic barrier for protecting metal corrosion. However, the industrial-scale application of alkanethiol SAMs is subject to some problems, such as alkanethiol having a peculiar smell and being usually insoluble in water. In aqueous solutions, the length of the alkane chain decreases the solubility of thiols. Therefore, an organic solvent is often used to dilute alkanethiol in the self-assembly process, resulting in environmental and safety problems. In addition, it also has been found that commonly used organic solvents, such as ethanol, harm the quality of SAMs. Over the past few years, waterborne[6] and supercritical CO_2-borne[7,8] strategies have been developed to replace organic solvents to obtain an eco-friendly film.

In water, hydrophobic alkanethiol spontaneously stratifies at the air interface. The addition of surfactants results in micelle formation around the alkanethiol molecule and aids in its diffusion to the metal surface.[9,10] Studies[11–14] by Yan *et al.* indicate that the selection of surfactants determined the micellar-borne SAMs on gold. Ganesh *et al.*[15,16] concluded that the micellar-borne SAMs have denser molecular packing and higher corrosion protection than SAMs formed in dichloromethane solvent. Raya *et al.*[17] also reported that the micellar-borne SAMs were included quickly and displayed better electron-transfer blocking properties. Liang *et al.*[18] investigated the anti-tarnishing ability of silver protected by the micellar-borne octadecanethiol (OT) with different surfactants. Wang *et al.*[19,20] revealed that the micellar-borne SAMs had comparable properties to those formed in ethanol. Wu *et al.*[21] investigated the dodecanethiol SAMs on copper from aqueous micellar solutions with CTAB surfactant and found that CTAB molecules were trapped into dodecanethiol (DT) SAMs. K. Ono *et al.*[22] also revealed that the corrosion resistance of OT SAMs for the electroless Au/Ni–P layer obtained in an aqueous micellar solution with a non-ionic surfactant was equivalent to that of SAMs from ethanolic solutions. On the other hand, organothiol with hydrophilic groups may be soluble in an aqueous solvent.[23] In this regard, Canaria *et al.*[24] prepared SAMs on gold in an aqueous solution without surfactant-aid using an amphipathic organothiol, structurally composed of an *n*-alkane chain with a thiol group at one end and a hydrophilic triethylene glycol group at the other end. However, to the best of our knowledge, reports on corrosion protection studies associated with

School of Materials Science and Engineering, Jiangxi Provincial Engineering Research Center for Surface Technology of Aeronautical Materials, Nanchang Hangkong University, Nanchang 330063, China. E-mail: pengshs@nchu.edu.cn
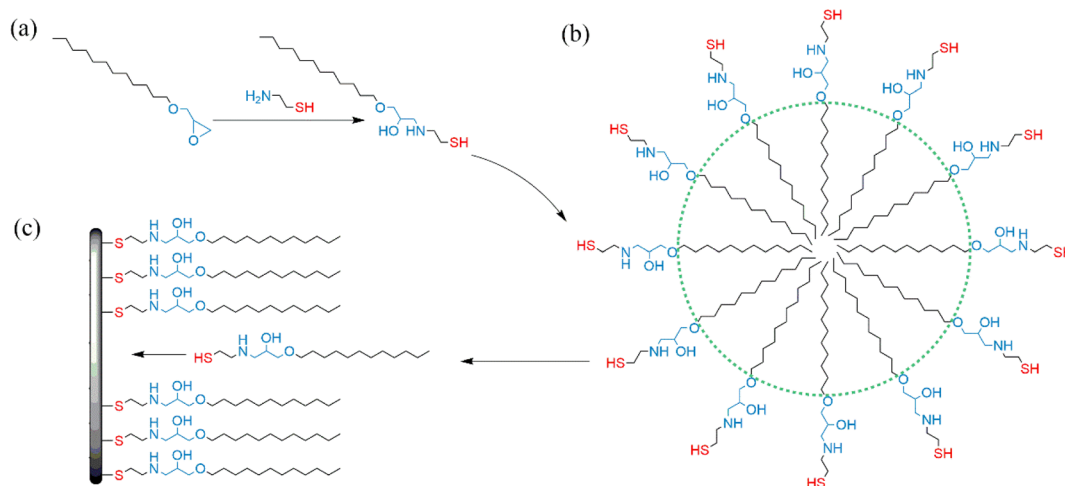
Fig. 1 Schematic diagram of (a) the reaction for synthesizing AGE-CA, (b) forming an AGE-CA emulsion, and (c) self-assembly of AGE-CA molecules on metal surfaces.

micellar-borne SAMs using an amphipathic organothiol are limited.

Cysteamine, containing both thiol and amine groups, has attracted the attention of many researchers and proved to be a suitable corrosion inhibitor for metals.[25,26] Burleigh *et al.*[27] claimed that fluorinated amidethiols synthesized from fluoroalkyl acid chloride and cysteamine have a very low mercaptan odor, unlike conventional alkanethiols used to protect the metal. Herein, we envisioned that an odorless amphipathic organothiol might reveal industrial-scale application and enhanced corrosion protection of SAMs for metals from an aqueous solution without surfactants. Therefore, in this work, we present the first report about the feasibility of preparing SAMs on nickel surfaces in an aqueous solution using an amphipathic organothiol (AGE-CA), which is synthesized by reacting C12–14 alkyl glycidyl ether (AGE) and cysteamine (CA). This amphipathic organothiol can anchor to metal surfaces through the terminal thiol group, and the C12–14 alkyl chain can form a hydrophobic protective layer. Moreover, the hydrophilic chain from the –NH$_2$ and glycidyl group reaction can endow the AGE-CA molecule with the self-emulsifying property. Different methods were used to characterize the resulting AGE-CA SAMs on nickel, and their protective properties were compared with those of the octadecanethiol SAMs prepared in ethanol solution Fig. 1.

2. Experimental

2.1 Chemicals

Octadecanethiol (OT), cysteamine, and C12-14 alkyl glycidyl ether are commercially available from Shanghai Aladdin Biochemical Technology Co., Ltd. All the other reagents are of chemical grade.

2.2 Preparation of AGE-CA

0.2 mol AGE and 0.1 mol cysteamine are dissolved in 100 ml of absolute ethanol, respectively. Then the two solutions are mixed evenly and reacted at 60 °C under stirring. After the reaction, ethanol is removed by rotary evaporation to obtain a colorless viscous liquid product (AGE-CA).

2.3 Preparation of aqueous micellar solutions of AGE-CA

1 g AGE-CA is poured into 100 ml deionized water, and the pH value is adjusted to 5.5 with acetic acid. This solution is dispersed by ultrasound for 10 minutes, and an opaque solution is finally obtained (Fig. 2).

2.4 Preparation of copper electrodes

A nickel rod with a diameter of 1 cm is soldered with Cu-wire for electrical connections and mounted into epoxy resin. Electrodes are polished with successive grades of SiC-type emery papers. Then the working electrodes are etched in 10% H$_2$SO$_4$ solution for 30 s and rinsed with distilled water immediately. Next, the

Fig. 2 Optical photos of AGE-CA self-emulsifying solution after six months at room temperature.

electrodes were immersed into the aqueous micellar solution of AGE-CA at room temperature for the designated time. Upon removal, the samples were washed with water and dried with nitrogen. For comparison, OT SAMs formed in 1 wt% OT ethanol solution at room temperature were also prepared.

The compositions of the nickel-plating baths used in this study were as follows: 250–300 g L^{-1} nickel sulfate, 35–40 g L^{-1} boric acid, 30–50 g L^{-1} nickel chloride, 0.05–0.10 sodium dodecyl sulfate, and pH 3.8–4.5. The nickel films are deposited on carbon steel at room temperature with a current density of 1.0–2.5 A dm^{-2} for about 10 min.

2.5 Characterization

The scanning range of FT-IR is 4000–400 cm^{-1}, and the scanning rate is 4 cm^{-1} s^{-1}. Liquid samples were dropped onto dry KBr sheets, and solid samples were ground with KBr into powder and pressed into sheets (1 mg of sample was added to 100 mg of KBr).

XPS revealed the surface chemical interaction between organic thiols and copper surfaces. XPS measurements were performed with an X-ray photoelectron spectrometer (AXISUL-TRA) manufactured by KRATOS, UK. The C1s central peak was shifted to 284.7 eV for correction to compensate for the binding energy offset caused by the sample surface charge, and the peak fitting was automatically processed using Casa XPS software.

3. Results and discussion

3.1 IR measurements

Fig. 3 shows the FT-IR spectra of CA, AGE, and the reaction product. For AGE, epoxide ring peaks at 3045, 1263, and 907 cm^{-1} are visible. Among those peaks, the most important one is the peak at 907 cm^{-1}, which is very strong and allows for monitoring of the reaction of the epoxy group.[28] As shown in Fig. 3, the peak at 907 cm^{-1} disappears from the IR spectra of the AGE-CA sample. According to a previous report, it can be known that the bending peak of N–H is 1521 cm^{-1}. Thus, the absence of the peak at 1521 cm^{-1} indicates that CA has a complete reaction with the epoxy group. Those results of IR analysis demonstrate that, in this case, the possible reaction between CA and AGE is a 1 : 2 adduct reaction between the N–H of CA and the epoxy group of the AGE molecule.

3.2 Effect of self-assembly time on the film properties

Fig. 4 shows the OCP curves of Ni electrodes in 3.5 wt% NaCl solution without and with AGE-CA. For the nickel electrode in the blank NaCl solution, the potential gradually increased from −0.258 V at the beginning and reached the maximum value of −0.229 V at about 25 min. Then the potential decays with a small amplitude, and the potential is −0.231 V after 120 min. The appearance of a potential peak at about 25 min may be related to the formation of nickel surface oxide. The subsequent possible decay is attributed to the chemical dissolution of nickel oxide, but this process is relatively slow, indicating that the dense oxide layer formed acts as a protective substrate and prevents further corrosion of the nickel surface in the NaCl
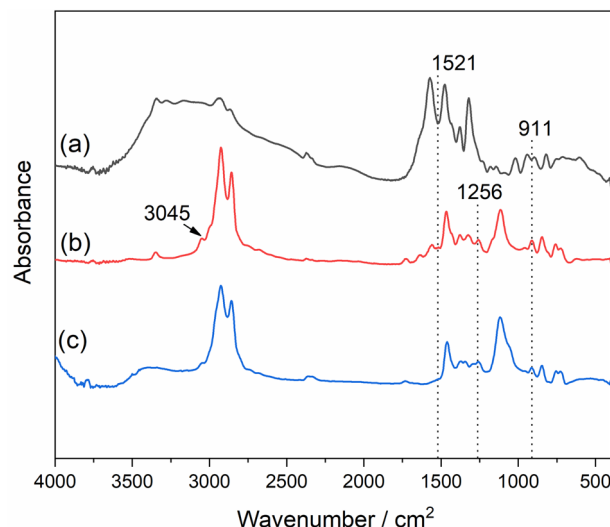

Fig. 3 FT-IR spectra of (a) CA, (b) AGE, and (c) the reaction product AGE-CA.

solution. In the NaCl solution containing AGE-CA, the potential increased from −0.262 V at the beginning to −0.217 V at 120 min. This may be because the thiol group of AGE-CA reacted with the nickel, and an AGE-CA film was formed on the nickel surface. The potential did not proliferate in the solution with AGE-CA before 50 min and was lower than in the blank solution. Subsequently, the potential still increases slowly and tends to be stable without a trend of decay, indicating that the formation of AGE-CA SAMs becomes more compact with immersion time prolonged. The OCP curve initially proves that the synthesized compound AGE-CA can form a protective film on nickel.

Fig. 5 presents the Tafel curves of the bare Ni and the Ni electrodes treated with different immersion times in the self-micellar AGE-CA solution. The anodic Tafel curve for the bare Ni electrode has a linear region. The apparent Tafel slope indicates mixed mass transfer and kinetic control.[29] Fig. 5
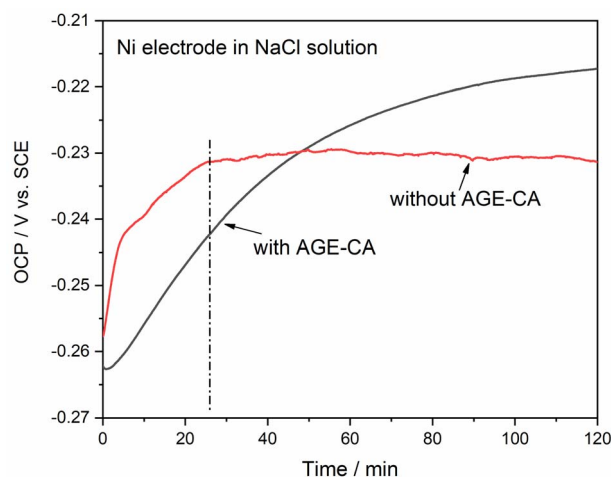

Fig. 4 Open potential curves of the Ni electrode in 3.5 wt% NaCl solution without and with AGE-CA.

demonstrates that both the anodic and cathodic current densities of the Ni electrodes are reduced significantly, and the suppression increases with prolonged treatment time. After self-assembly for 1 h, the current densities are cut down by two orders of magnitude.

According to the Tafel curves, the corrosion current density (i_{corr}) can be calculated by extrapolating the linear Tafel section of the anode and cathode curves to the corrosion potential (E_{corr}), and the fitting parameters are presented in Table 1. The following equation calculates the inhibition efficiency (η):

$$\eta = \left(1 - \frac{i_{corr}}{i_{corr}^0}\right) \times 100\%$$

wherein i_{corr}^0 and i_{corr} are the corrosion current densities of the bare and modified nickel electrode, respectively. The results show that the η value of the Ni electrode treated for 30 min is about 61.1%. When the electrode is immersed for 60 min and 90 min, the η value increases to 89.3% and 96.4%, respectively. The high η value of SAMs against the corrosion of Ni may be attributed to the non-conductivity and hydrophobicity of alkanes in densely stacked AGE-CA molecules on the Ni surface. As the immersion time continued to prolong to 120 min, the η value slightly decreased to 93.2%, possibly due to the forming defects in SAMs caused by the AGE-CA molecular desorption.[19]

Fig. 6 shows the Nyquist diagrams obtained for the bare Ni electrode in a 3.5 wt% NaCl solution, diagrams that offer only one semi-circle in the range of the frequencies studied. The presence of this capacitive loop is attributed to the charge transfer process and the double-layer capacitance at the metal/solution interface; similar results were previously reported for Ni electrodes in NaCl solutions. The EIS results of the bare Ni can be analyzed with the equivalent circuit in Fig. 8, wherein R_s is the solution resistance, R_{ct} is the transfer resistance, and CPE is the constant phase element.

As shown in Fig. 7, the Nyquist plots of AGE-CA treated electrodes differ from those of the bare one in shape and size.

Table 1 Electrochemical parameters for the bare and SAM-covered Ni electrodes calculated from the Tafel curves

Sample	E_{corr} (V vs. SCE)	i_{corr} (A cm^{-2})	η
Bare	−0.271	3.09×10^{-6}	—
30 min	−0.222	1.21×10^{-6}	61.1%
60 min	−0.221	3.31×10^{-7}	89.3%
100 min	−0.224	8.09×10^{-8}	97.4%
120 min	−0.219	2.08×10^{-7}	93.2%

With the increase of immersion time, the increasing diameter of the Nyquist semi-circle indicates that AGE-CA SAMs significantly but gradually change the corrosion kinetics of the Ni surface, which means that the formation of AGE-CA SAMs changes the electrode interfacial structure. In the case of long immersion time, reflecting that the SAMs have a good inhibition effect, they can prevent the diffusion processes of the ions. It is reasonable to analyze these plots with the equivalent circuit in Fig. 8. R_{ct} stands for the transfer resistance of electrons through the monolayers, and Q_f represents the capacitance of the SAMs.

The values of the elements of the equivalent circuits obtained by fitting are given in Table 2. The listed surface coverage (θ) is calculated with the following formula:

$$\theta = 1 - \frac{R_{ct}^0}{R_{ct}}$$

wherein R_{ct}^0 is the charge transfer resistance of the bare Ni electrode and R_{ct} is the charge transfer resistance of the corresponding SAM-covered electrodes. Here, R_f is used instead of R_{ct} to calculate the surface coverage. Compared with the inhibition efficiency obtained from the Tafel study, the values of θ are almost identical to those of η. For example, the θ and η values obtained after self-assembly for 90 min are 98.2% and 97.4%, respectively.
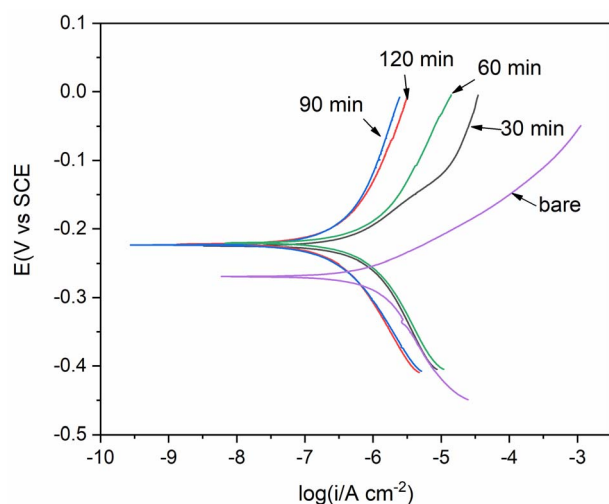
Fig. 5 The Tafel curves of the bare Ni and the electrodes treated with different immersion times in the self-micellar AGE–CA solution.
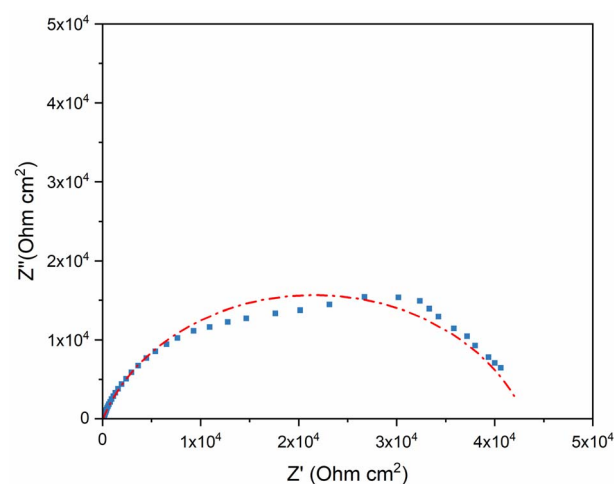
Fig. 6 The Nyquist plots of the bare Ni electrodes measured in a 3.5 wt% NaCl solution.
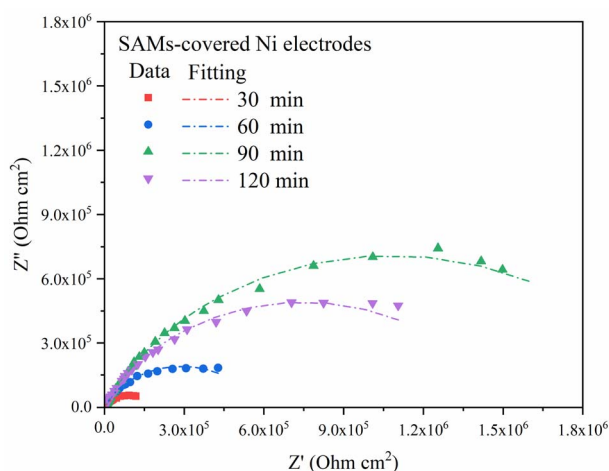
Fig. 7 The Nyquist plots of the Ni electrodes treated with different immersion times in the self-micellar AGE-CA solution.
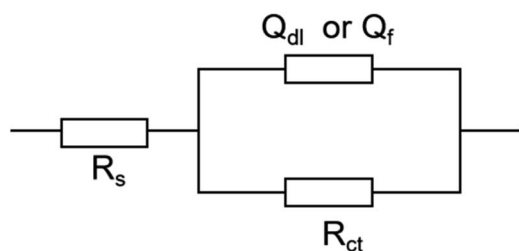

Fig. 8 The equivalent circuits for bare and AGE-CA treated Ni electrodes.

According to the above studies, high-quality SAMs can be assembled in the AGE-CA emulsion for 90 min. Cyclic voltammetry (CV) provides valuable information on the electrochemical stability and charge behavior of oxidation and reduction reactions on Ni electrodes in solution. As seen in Fig. 9a, the bare Ni electrodes show that the anode current increases sharply during the first cycle from −0.07 V and decreases rapidly at the first return potential. In the subsequent cathodic scan, no current peak corresponding to the anode is found, which is caused by the formation of an oxide layer on the nickel surface, leading to passivation.[30] During the second cycle, a small current peak at 0.12 V appeared on the anode, and then the current density increased at 0.16 V, indicating that the Ni

surface was further oxidized.[31] The anode current in the fourth cycle decreased by magnitude compared with that in the first cycle, indicating that the oxide film covering the nickel surface was gradually dense, and the contact between chloride ions and nickel substance was hindered. In the cathodic scan, there is no current peak, and the cathode current almost does not change with the increase of the number of cycles, indicating that the dense oxide layer covering the nickel surface in NaCl solution has not been reduced to nickel metal. Fig. 9b shows no oxidation peak interval in the anode process, indicating that the AGE-CA film inhibits the oxidation of the nickel surface. The current density of the anode and cathode is significantly reduced, indicating that the film is relatively dense and the AGE-CA molecule has a strong interaction with the nickel surface.

3.3 XPS

XPS was used to investigate the Ni surface oxidation and AGE-CA chemisorption. Fig. 10 shows the survey spectra of bare and the AGE-CA modified Ni. For AGE-CA modified nickel, the presence of N 1s and S 2p binding energies indicates that AGE-CA molecules have been successfully assembled on the nickel surface. The binding energies of about 853.8 eV and 874.4 eV are
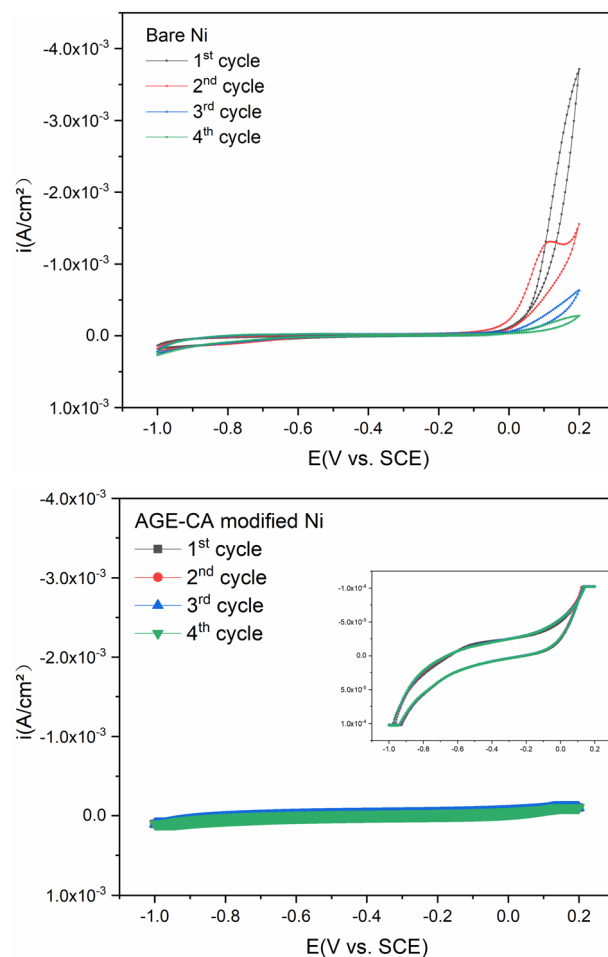

Fig. 9 Cyclic voltammetry of bare and AGE-CA modified Ni electrodes in 3.5 wt% NaCl solution with a scan rate of 0.01 V s⁻¹.

Table 2 The equivalent circuits parameters of the bare and SAM-covered Ni electrodes calculated from EIS; electrochemical parameters and surface coverage (θ) of bare Ni and the electrodes treated with different immersion times in the self-micellar AGE-CA solution

	Q ($S\ s^n\ 10^{-6}$)	n_{dl}	R_{ct} (Ohm cm²)	θ
bare	78.5	0.80	8.61×10^3	—
30 min	2.31	0.90	2.33×10^4	63.1
60 min	0.61	0.93	1.11×10^5	92.3
90 min	0.12	0.97	5.56×10^5	98.2
120 min	0.37	0.98	1.81×10^5	95.3

attributed to Ni 2p3/2 and Ni 2p1/2, respectively. Compared with the bare Ni, the relative intensity of the two peaks in the modified Ni was significantly reduced. This indicated that the metal oxides on the AGE-CA modified nickel surface are
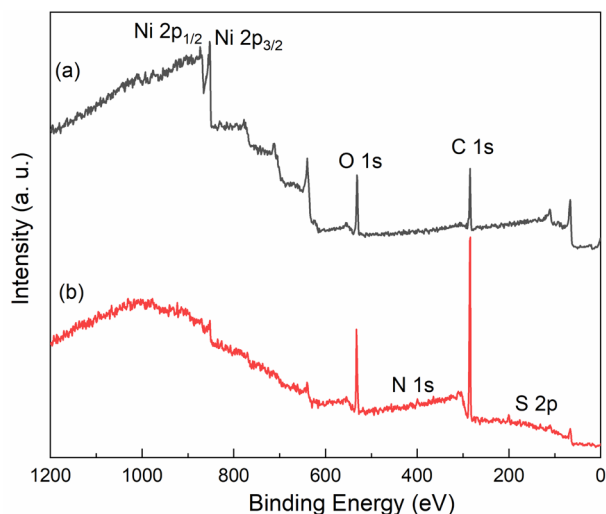

Fig. 10 The survey spectra of (a) bare Ni and (b) AGE-CA modified Ni.
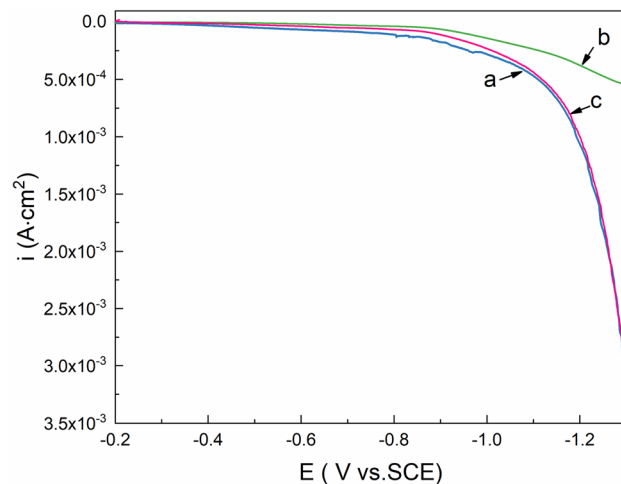

Fig. 12 LSV of Ni electrodes in 3.5 wt% solutions: (a) bare, (b) with AGE-CA SAMs, and (c) with DT SAMs.

reduced. Fig. 11 shows the high-resolution spectra. The O 1s peak with a binding energy of about 529.1 eV can be attributed to the Ni–O bond. The relative strength of this peak is significantly reduced in the modified Ni, which further indicates that
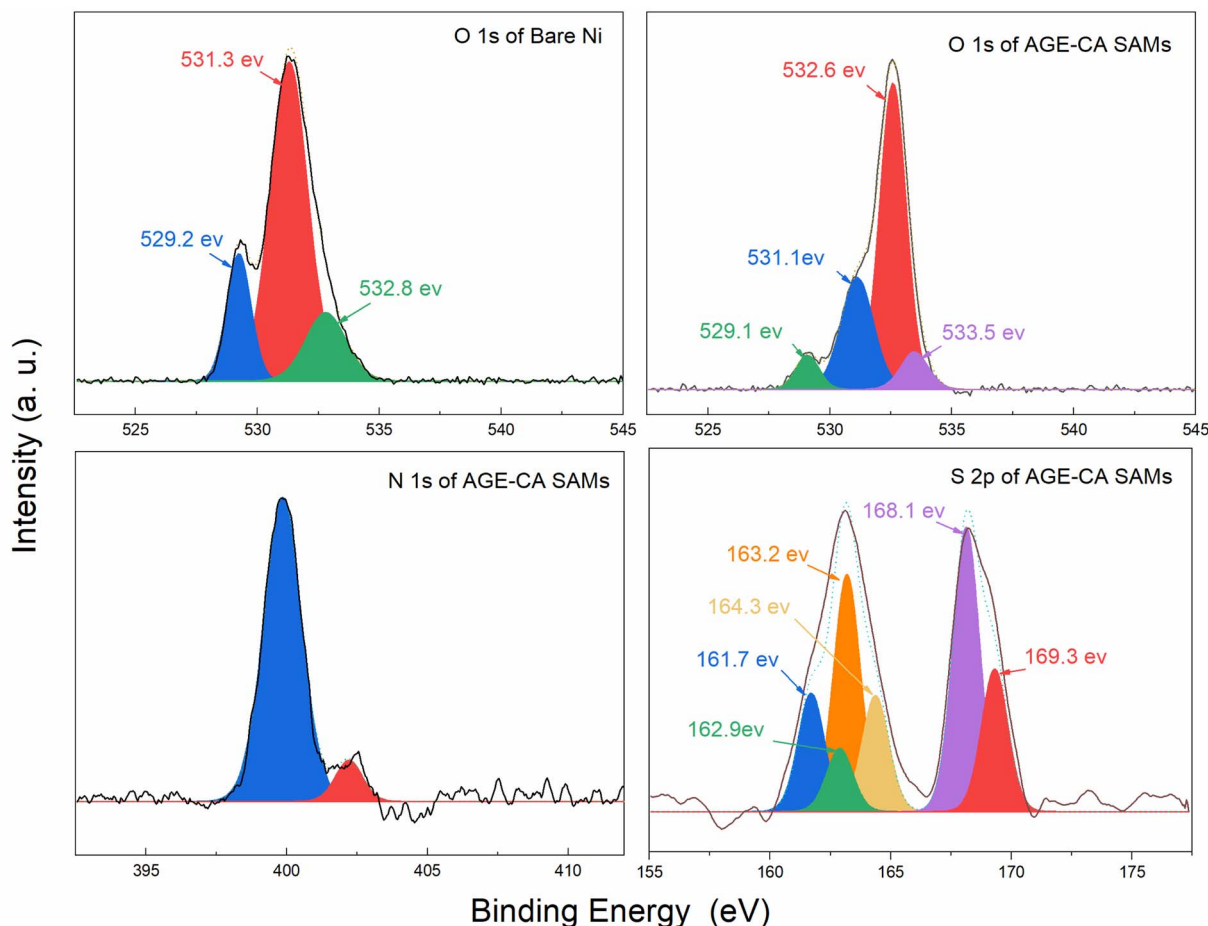

Fig. 11 Full resolution XPS: O 1s for bare Ni, and O 1s, N 1s, and S 2p for AGE-CA SAM-covered Ni.
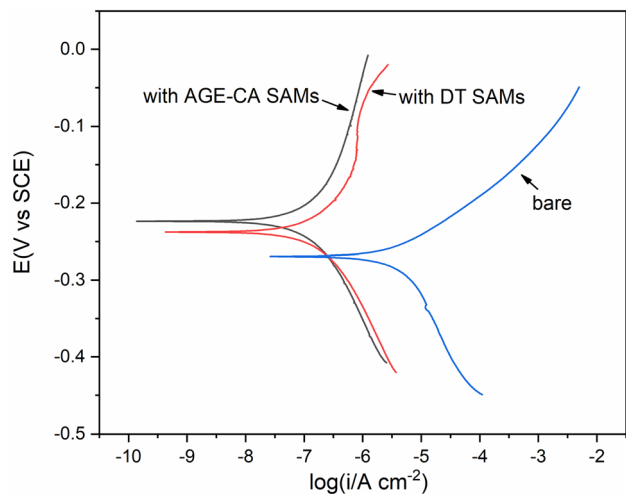
Fig. 13 The Tafel curves of bare and SAM-covered Ni electrodes in 3.5 wt% solutions.

the AGE-CA SAMs inhibit the production of nickel oxide. The O 1s peak can be convoluted to C–O–C (532.6 eV) and –OH (533.6 eV), which are unique structures of AGE-CA. The binding energy of the chemisorbed S 2p3/2 component on nickel ranges from 161.8 to 163.3 eV.[32] The binding energy of the S atom in the Ni–S form ranges from 161.0 to 162.2 eV.[33] Thus, the peak of about

161.7 eV in Fig. 10 can be attributed to the Ni–S bond. XPS analysis shows that AGE-CA is successfully adsorbed on the Ni surface to form SAMs.

3.4 Comparison of the properties of the AGE-CA SAMs and OT SAMs

To investigate the differences between the AGE-CA SAMs formed in an aqueous micellar solution and the DT SAMs created in an ethanol solution, Ni electrodes and plating Ni are assembled in the two kinds of solutions for 90 min.

Linear sweep voltammetry (LSV) was performed in 3.5 wt% NaCl solution, to determine the desorption behavior of AGE-CA SAMs on the Ni surface, relative to the reference electrode of −0.2–1.25 V. As shown in Fig. 12, for the bare Ni and DT SAM-covered electrode, when the potential reaches −1.1 V, the current densities increase suddenly, indicating that the oxide film and DT SAMs on the Ni surface have been damaged, respectively. For the AGE-CA SAM-covered electrode, when the potential reaches −1.2 V, the current density remains at a small value, which means that AGE-CA SAMs are firmly anchored on the Ni surface. Fig. 12 shows the Tafel curves of bare and SAM-covered Ni electrodes in 3.5 wt% solutions. It can be concluded from the figure that the AGE-CA SAMs from the aqueous self-emulsifying solution provide better protection for Ni than the OT SAMs from the ethanol solution (Fig. 13).

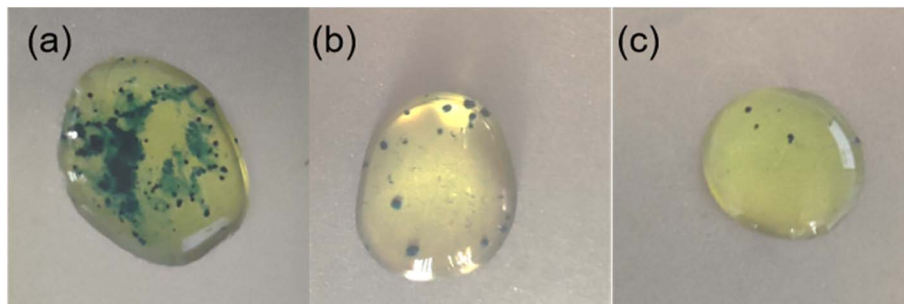**Fig. 14** Porosity test for electroplated Ni samples: (a) bare, (b) OT and (c) AGE–CA SAM-covered.
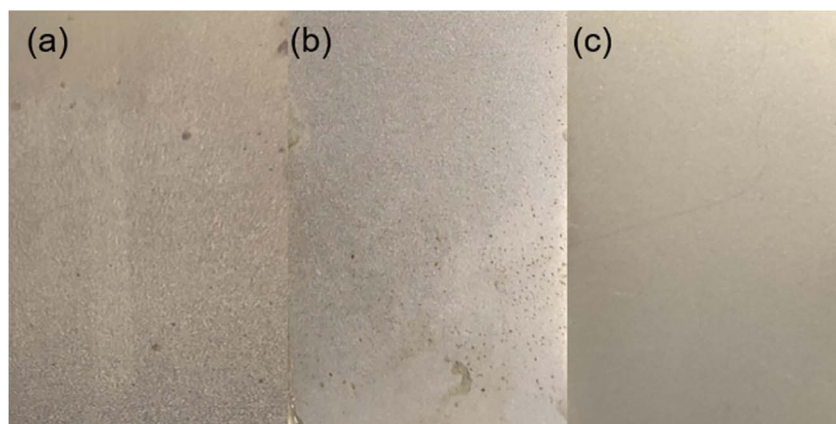

Fig. 15 Salt spray test of electroplated Ni samples: (a) bare (after 1 h), (b) with OT SAMs (after 2 h), and (c) with AGE–CA SAMs (after 8 h).

It was also found that AGE-CA SAMs could improve the corrosion resistance of the electroplated Ni coating on carbon steel. Fig. 14 shows the results of the porosity measurement. It can be seen that there are many green spots in the untreated electroplated Ni sample. The number of green sites for the electroplated Ni sample with OT SAMs is reduced, indicating that the DT SAMs could improve the corrosion resistance of the electroplated Ni coating. Surprisingly, the number of green spots for the AGE-CA SAM-covered sample is remarkably less than that for the OT SAM-covered one.

Fig. 15 presents the salt spray test results. As shown in Fig. 15, brown corrosion products appear on the surface of untreated samples after 1 h of the salt spray test. There are also evident corrosion traces on the surface after two hours of salt spray for OT SAM-covered samples. However, there is no visible corrosion trace on the surface of the AGE-CA SAM-covered samples after 8 hours of salt spray. These experiments verify that the AGE-CA SAMs significantly improve the corrosion resistance of the electroplated Ni film.

4. Conclusion

A novel amphiphilic organothiol was successfully prepared by cysteamine and C12-14 alkyl glycidyl ether. The as-prepared amphiphilic organothiol can self-emulsify and disperse in an aqueous solution to form a stable emulsion without any additional emulsifier. XPS results show that the as-prepared self-emulsifying organothiol can bond to the Ni surface by forming strong thiolate Ni–S bonds. The electrochemical measurements show that the η value and θ value increase with the immersion time in the aqueous micellar solution, reaching the maximum value of about 90 minutes. The electrochemical measurements, XPS, porosity tests, and neutral salt spray experiments prove that the AGE-CA SAMs from the self-emulsifying solution provided better protection for Ni substances and electroplated Ni film than the OT SAMs from the ethanol solution. The results suggest that the proposed self-emulsifying organothiol used to prepare SAMs is simple and environmentally friendly. Therefore, it has the potential to replace the conventional method.

Conflicts of interest

There are no conflicts to declare.

Acknowledgements

References

1 C. Vericat, M. E. Vela, G. Benitez, P. Carro and R. C. Salvarezza, Self-assembled monolayers of thiols and dithiols on gold: new challenges for a well-known system, *Chem. Soc. Rev.*, 2010, **39**(5), 1805–1834.

2 A. Ulman, Formation and structure of self-assembled monolayers, *Chem. Rev.*, 1996, **96**(4), 1533–1554.

3 P. E. Laibinis and G. M. Whitesides, Self-assembled monolayers of n-alkanethiolates on copper are barrier films that protect the metal against oxidation by air, *J. Am. Chem. Soc.*, 1992, **114**(23), 9022–9028.

4 S. Peng, W. Zhao, H. Li, Z. Zeng, Q. Xue and X. Wu, The enhancement of benzotriazole on epoxy functionalized silica sol-gel coating for copper protection, *Appl. Surf. Sci.*, 2013, **276**, 284–290.

5 Y. Tao, X. Chen, S. Peng and Y. Ma, The enhancement and mechanism of potential-assisted method on 2-mercaptobenzobthiazole assembled film for copper protection, *Colloids Surf., A*, 2022, **638**, 128280.

6 M. Byloos, H. Al-Maznai and M. Morin, Formation of a Self-Assembled Monolayer *via* the Electrospreading of Physisorbed Micelles of Thiolates, *J. Phys. Chem. B*, 1999, **103**(31), 6554–6561.

7 R. D. Weinstein, D. Yan and G. K. Jennings, Self-Assembled Monolayer Films from Liquid and Supercritical Carbon Dioxide, *Ind. Eng. Chem. Res.*, 2001, **40**(9), 2046–2053.

8 D. Yan, G. K. Jennings and R. D. Weinstein, Controlling the Properties of n-Alkanethiolate Self-Assembled Monolayers on Gold by Using Supercritical Carbon Dioxide–Ethanol Mixtures as Solvents, *Ind. Eng. Chem. Res.*, 2002, **41**(18), 4528–4533.

9 J. Liu and A. E. Kaifer, Preparation of Self-Assembled Monolayers from Micellar Solutions, *Isr. J. Chem.*, 1997, **37**(2–3), 235–239.

10 L. Patrone, S. Palacin, J.-P. Bourgoin and M. H. V. Werts, Versatility of Aqueous Micellar Solutions for Self-Assembled Monolayers Engineering, *Langmuir*, 2004, **20**(26), 11577–11582.

11 D. Yan, A. S. Jeremy and G. K. Jennings, Enhanced Chain Densities of n-Alkanethiolate Self-Assembled Monolayers on Gold from Aqueous Micellar Solutions, *Langmuir*, 2000, **16**(20), 7562–7565.

12 D. Yan, J. A. Saunders and G. K. Jennings, Kinetics of formation for n-alkanethiolate self-assembled monolayers onto gold in aqueous micellar solutions of C12E6 and C12E7, *Langmuir*, 2002, **18**(26), 10202–10212.

13 D. Yan, J. L. Jordan, V. Burapatana and G. K. Jennings, Formation of n-Alkanethiolate Self-Assembled Monolayers onto Gold in Aqueous Micellar Solutions of n-Alkyltrimethylammonium Bromides, *Langmuir*, 2003, **19**(8), 3357–3364.

14 D. Yan, A. S. Jeremy and G. K. Jennings, Formation and Stability of Hexadecanethiolate SAMs Prepared in Aqueous Micellar Solutions of C12E6, *Langmuir*, 2003, **19**(22), 9290–9296.

15 V. Ganesh, S. K. Pal, S. Kumar and V. Lakshminarayanan, Self-assembled monolayers (SAMs) of alkoxycyanobiphenyl thiols on gold surface using a lyotropic liquid crystalline medium, *Electrochim. Acta*, 2007, **52**(9), 2987–2997.

16 V. Ganesh and V. Lakshminarayanan, Self-Assembled Monolayers of Alkanethiols on Gold Prepared in a Hexagonal Lyotropic Liquid Crystalline Phase of Triton X-100/Water System, *Langmuir*, 2006, **22**(4), 1561–1570.

17 D. García Raya, R. Madueño, M. Blázquez and T. Pineda, Formation of a 1,8-Octanedithiol Self-Assembled Monolayer on Au(111) Prepared in a Lyotropic Liquid-Crystalline Medium, *Langmuir*, 2010, **26**(14), 11790–11796.

18 C. H. Liang, C. J. Yang and N. B. Huang, Tarnish protection of silver by octadecanethiol self-assembled monolayers prepared in aqueous micellar solution, *Surf. Coat. Technol.*, 2009, **203**(8), 1034–1044.

19 C. H. Liang, P. Wang, B. Wu, N. B. Huang and J. L. Li, Protection of copper corrosion by modification of dodecanethiol self-assembled monolayers prepared in aqueous micellar solution, *Electrochim. Acta*, 2010, **55**(3), 878–883.

20 P. Wang, C. Liang and N. Huang, Studies on corrosion inhibition of copper by alkanethiol SAMs prepared in aqueous micellar solution, *Mater. Corros. - Werkst. Korros.*, 2010, **61**(4), 332–337.

21 S. S. Wu, Z. Y. Chen, Y. B. Qiu and X. P. Guo, Corrosion Protection of Copper by Self-Assembled Monolayers Modified in Aqueous Micellar Solution, *J. Electrochem. Soc.*, 2012, **159**(7), C277–C282.

22 K. Ono, T. Kurashina, K. Takahashi and N. Kodama, Practical Use of 1-octadecanethiol Self-assembly Monolayers Obtained from Aqueous Micellar Solution as Corrosion Inhibitor for Printed Wiring Boards, *J. Surf. Finish. Soc. Jpn.*, 2013, **64**(2), 140–145.

23 M. Riepl, K. Enander, B. O. Liedberg, M. Schäferling, M. Kruschina and F. Ortigao, Functionalized Surfaces of Mixed Alkanethiols on Gold as a Platform for Oligonucleotide Microarrays, *Langmuir*, 2002, **18**(18), 7016–7023.

24 C. A. Canaria, J. So, J. R. Maloney, C. J. Yu, J. O. Smith, M. L. Roukes, S. E. Fraser and R. Lansford, Formation and removal of alkylthiolate self-assembled monolayers on gold in aqueous solutions, *Lab Chip*, 2006, **6**(2), 289–295.

25 P. Song, X.-Y. Guo, Y. C. Pan, S. Shen, Y. Sun, Y. Wen and H.-F. Yang, Insight in cysteamine adsorption behaviors on the copper surface by electrochemistry and Raman spectroscopy, *Electrochim. Acta*, 2013, **89**, 503–509.

26 N. Karthik and M. G. Sethuraman, Assessment of the corrosion protection ability of cysteamine and hybrid sol–gel twin layers on copper in 1% NaCl, *RSC Adv.*, 2015, **5**(12), 8693–8705.

27 T. D. Burleigh, C. Shi, S. Kilic, S. Kovacik, T. Thompson and R. M. Enick, Self-Assembled Monolayers of Perfluoroalkyl Amideethanethiols, Fluoroalkylthiols, and Alkylthiols for the Prevention of Silver Tarnish, *Corrosion*, 2002, **58**(1), 49–56.

28 S. Peng, Z. Zeng, W. Zhao, H. Li, Q. Xue and X. Wu, Synergistic effect of thiourea in epoxy functionalized silica sol–gel coating for copper protection, *Surf. Coat. Technol.*, 2012, **213**, 175–192.

29 S. Peng, Z. Zeng, W. Zhao, H. Li, Q. Xue and X. Wu, The enhancement of benzotriazole on epoxy functionalized silica sol–gel coating for copper protection, *Appl. Surf. Sci.*, 2013, **276**, 284–290.

30 Z. Mekhalif, J. Riga, J. J. Pireaux and J. Delhalle, Self-Assembled Monolayers of n-Dodecanethiol on Electrochemically Modified Polycrystalline Nickel Surfaces, *Langmuir*, 1997, **13**(8), 2285–2290.

31 T. S. Rufael, D. R. Huntley, D. R. Mullins and J. L. Gland, Adsorption and Reaction of Dimethyl Disulfide on the Ni(111) Surface, *J. Phys. Chem. B*, 1998, **102**(18), 3431–3440.

32 D. R. Mullins, T. Tang, X. Chen, V. Shneerson and W. T. Tysoe, The adsorption site and orientation of CH_3S and sulfur on Ni(001) using angle-resolved X-ray photoelectron spectroscopy, *Surf. Sci.*, 1997, **372**(1–3), 193–201.

33 H. Hu, M. Qiao, F. Xie, K. Fan, H. Lei, D. Tan, X. Bao, H. Lin, B. Zong and X. Zhang, Comparative X-ray photoelectron spectroscopic study on the desulfurization of thiophene by Raney Nickel and rapidly quenched skeletal nickel, *J. Phys. Chem. B*, 2005, **109**(11), 5186–5192.